

## REHABILITATION

# Robot-induced perturbations of human walking reveal a selective generation of motor adaptation

Iahn Cajigas,<sup>1\*</sup> Alexander Koenig,<sup>1\*</sup> Giacomo Severini,<sup>1,2\*</sup> Maurice Smith,<sup>3</sup> Paolo Bonato<sup>1,4†</sup>

2017 © The Authors,  
some rights reserved;  
exclusive licensee  
American Association  
for the Advancement  
of Science.

The processes underlying the generation of motor adaptation in response to mechanical perturbations during human walking have been subject to debate. We used a robotic system to apply mechanical perturbations to step length and step height over consecutive gait cycles. Specifically, we studied perturbations affecting only step length, only step height, and step length and height in combination. Both step-length and step-height perturbations disrupt normal walking patterns, but step-length perturbations have a far greater impact on locomotor stability. We found a selective process of motor adaptation in that participants failed to adapt to step-height perturbations but strongly adapted to step-length perturbations, even when these adaptations increased metabolic cost. These results indicate that motor adaptation during human walking is primarily driven by locomotor stability, and only secondarily by energy expenditure and walking pattern preservation. These findings have substantial implications for the design of protocols for robot-assisted gait rehabilitation.

## INTRODUCTION

Previous studies have investigated how human subjects adapt motor plans in response to sudden or gradual changes in the environment. These studies have often referred to Shadmehr and Mussa-Ivaldi's seminal work on upper-limb motor adaptation (1). The authors used a robotic manipulandum to produce a velocity-dependent force and affect subjects' upper-limb point-to-point movements. Study participants showed motor adaptation countering the predicted effect of the robot-produced force, hence suggesting the generation of error-driven adjustments derived from internal models. The central nervous system (CNS) uses such models to predict the outcome of a given motor plan in the task space in which the experiment takes place (2–4). Several investigators have proposed experimental paradigms to extend Shadmehr and Mussa-Ivaldi's study to the lower limbs either by using robotic systems to produce external forces as a means to produce a mechanical perturbation (5–10) or by relying upon treadmill walking-based protocols to create the conditions in which motor adaptation could be observed (11–15).

Emken and Reinkensmeyer (5), van Asseldonk *et al.* (7), and our own research group (8) used robotic systems to generate forces affecting the foot trajectory of one leg during treadmill walking. Emken and Reinkensmeyer (5) interpreted motor adaptation in response to a velocity-dependent upward force during the swing phase of the gait cycle as the result of a trade-off between restoring the baseline foot trajectory and minimizing the metabolic cost of locomotion (6). van Asseldonk *et al.* (7) studied the response to sudden and gradual downward forces produced during the swing phase. The authors interpreted the responses to sudden forces as aimed to assure locomotor stability and the responses to gradual forces as a strategy to preserve baseline foot trajectory. Our own work (8) showed responses to mechanical perturbations orthogonal to the trajectory of

movement in the joint coordinate space (i.e., knee versus hip angle). We argued that the experimental observations reflected a bias toward maintaining the baseline trajectory of movement. Lam *et al.* (9) and Selinger *et al.* (10) used robotic systems to produce resistive forces during the swing phase. Lam *et al.* (9) observed rapid changes in the electromyographic activity consistent with feedback mechanisms aimed to assure locomotor stability and slow changes consistent with feed-forward mechanisms to restore baseline kinematics. Selinger *et al.* (10) used robotic knee braces to produce a resistive torque that varied with the step frequency. They observed that subjects adjusted their step frequency to achieve minimum metabolic cost of locomotion.

Prokop *et al.* (11), Reisman *et al.* (12), and Choi and Bastian (13) used a split-belt treadmill to study motor behaviors when the belts were moved at different speeds or in different directions. Prokop *et al.* (11) argued that changes in the interlimb coordination observed when the belts were moved at different speeds were primarily caused by the need for assuring locomotor stability. Reisman *et al.* (12) looked upon motor adaptation when subjects walked with the belts moving at different speeds as associated with optimal locomotor stability and metabolic cost of locomotion. Choi and Bastian (13) tested subjects during backward and hybrid walking (i.e., walking forward with one leg and backward with the other). They observed motor adaptation that was leg- and direction-specific. They suggested that interlimb coordination is the result of a synchronized modulation of the activity of leg-specific locomotor networks. Savin *et al.* (14) used a single-belt treadmill and studied motor adaptation by connecting/disconnecting a weight to one leg using a pulley. They observed bilateral adaptation and suggested that motor adaptation should be considered in the context of the goals and task constraints associated with the experiment rather than as indicative of the relevance of interlimb over intralimb control. Last, Finley *et al.* (15) demonstrated that there is a linear relationship between the time course of the motor adaptation and the metabolic cost of walking.

This body of work points at three potential principles used by the CNS to generate lower limb motor adaptation: (i) maintaining the gait patterns observed in the absence of perturbations, (ii) minimizing the metabolic cost of locomotion, and (iii) preserving locomotor stability. However, the substantial differences in motor adaptation

<sup>1</sup>Department of Physical Medicine and Rehabilitation, Harvard Medical School, 300 First Avenue, Charlestown, MA 02129, USA <sup>2</sup>School of Electrical and Electronic Engineering, University College Dublin, Belfield, Dublin 4, Ireland. <sup>3</sup>School of Engineering and Applied Science, Harvard University, 29 Oxford Street, Cambridge, MA 02138, USA. <sup>4</sup>Wyss Institute for Biologically Inspired Engineering, Harvard University, 3 Blackfan Circle, Boston, MA 02115, USA.

\*These authors contributed equally to this work.

†Corresponding author. Email: pbonato@mgh.harvard.edu

observed under different experimental constraints and our limited understanding of the interplay among the principles used by the CNS to generate motor adaptation make it difficult to predict how patients would respond to the interaction with a robotic system for gait rehabilitation. Here, we present the results of a systematic study on the effects of mechanical perturbations produced using an exoskeleton system for treadmill-based gait rehabilitation (Lokomat by Hocoma AG, Zurich, Switzerland) (Fig. 1A). This work was motivated by the observation that the modification of gait patterns is an important goal of physical therapy and that the study of motor adaptation has significant potential for assessing the ability of patients to modify their gait patterns (16). Our work was focused on characterizing motor adaptation in healthy subjects as a necessary step before motor adaptation could be investigated in patients. Study volunteers were instructed to walk at 3 km/hour at a pace of about 86 steps per minute. The system produced mechanical perturbations that were applied to the subjects' right lower limb during the swing phase of the gait cycles. Tests were performed using the robotic system to produce net perturbation forces (herein referred to as perturbation force vectors) at the foot with different orientations in the

sagittal plane. We hypothesized that we would have observed motor adaptation for all the orientations of the perturbation force vector should the underlying goal of the CNS be to preserve only baseline gait kinematics. To our surprise, the results of the study revealed instead a selective process of generation of motor adaptation.

**RESULTS**

We performed two sets of experiments. The first set of experiments was focused on assessing the biomechanical effects of robot-induced perturbations applied over nonconsecutive gait cycles. We refer to these perturbations as single-step perturbations. The second set of experiments was designed to study whether healthy subjects adapt to mechanical perturbations applied over consecutive gait cycles. We refer to this second set of experiments as motor adaptation experiments.

**Single-step perturbation experiments**

Single-step perturbations were induced by the robot for one randomly selected gait cycle every 10 cycles. They were generated using

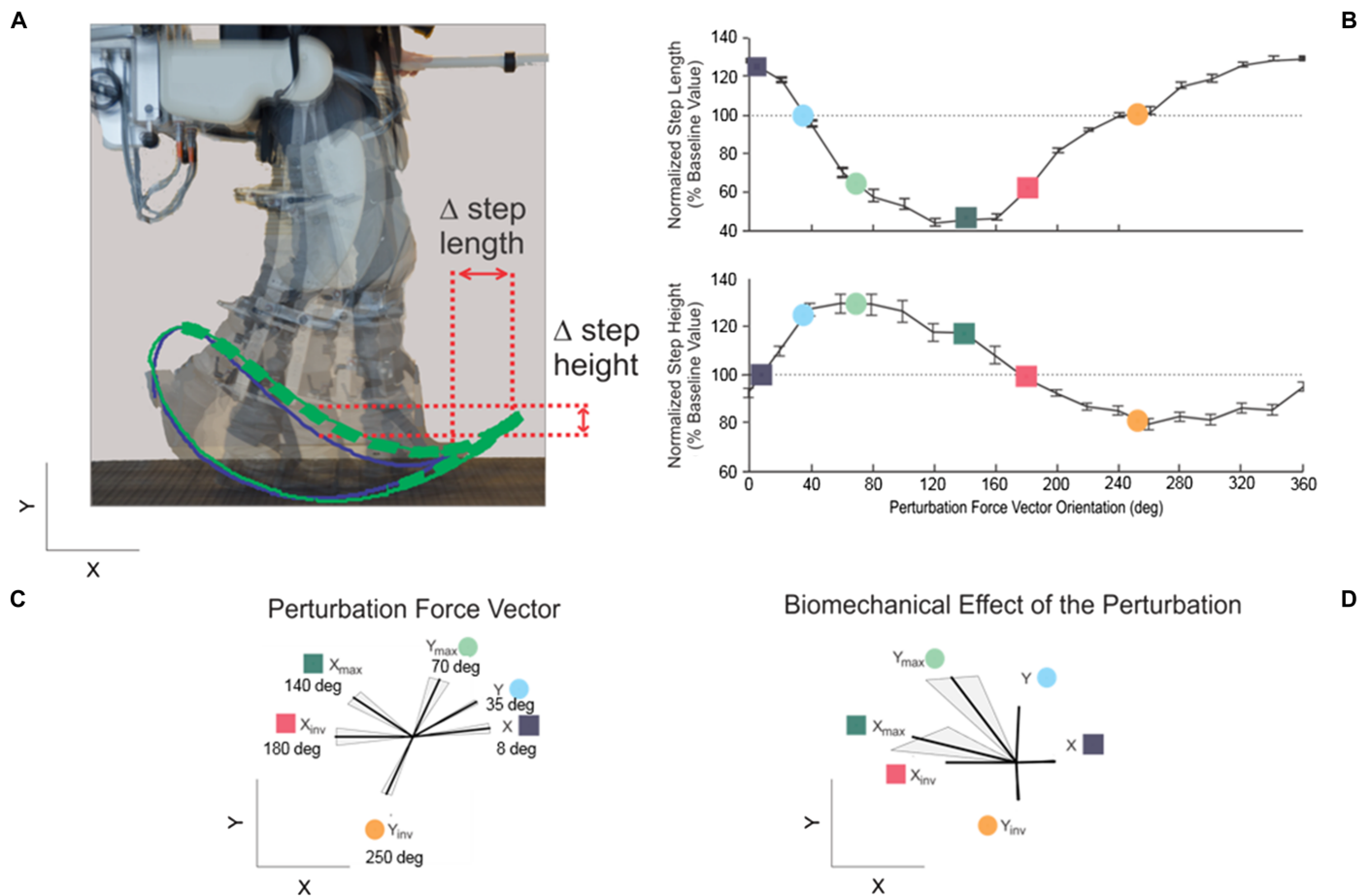


**Fig. 1. Schematic representation of the effects of the mechanical perturbations generated by the robot used in the study.** (A) The robot was used to cause the foot trajectory to change (green line) compared with baseline (blue line). Forces were generated by the robot during a portion of the gait cycle approximately corresponding to the swing phase (bold dashed green line). Step-length and step-height values were estimated during the perturbation phase of the experiments and compared with baseline values. (B) Results of the single-step perturbation experiments for step length and step height. The bottom plots show the orientation of the perturbation force vectors selected for the motor adaptation experiments (C) and their biomechanical effects on step length and step height (D). The shaded areas in (C) show the variability across subjects (i.e., SE) in the orientation of the vectors that resulted in the desired effects (i.e.,  $X_{inv}$ ,  $Y_{inv}$ ,  $X_{max}$ , and  $Y_{max}$ ). The shaded areas in (D) show the variability across subjects in the resultant biomechanical effect (i.e., effects on step length and step height).

the hip and knee actuators of the robot's right leg to result in a net force (herein referred to as perturbation force vector) at the distal end of the robotic leg that affected the foot trajectory. We tested the effect of 19 different orientations of the perturbation force vector in the sagittal plane ranging from  $0^\circ$  to  $360^\circ$  by increments of  $20^\circ$  (with the vectors at  $0^\circ$  and  $360^\circ$  oriented horizontally in the forward direction). This set of experiments allowed us to evaluate the effects of the orientation of the perturbation force vector. Our analyses focused on changes in step length and step height.

Figure 1 shows the results of the single-step perturbation experiments performed in 15 study volunteers. Figure 1B shows the group average and standard error of the normalized step-length and step-height values observed for the gait cycles during which mechanical perturbations were applied by the robot. The step-length and step-height values were normalized by the average step-length and step-height values observed when no perturbations were present.

When plotted as a function of the orientation of the perturbation force vector, the normalized step-length and step-height values showed a nonsymmetric but roughly sinusoidal pattern. Interpolation of the experimental results allowed us to choose values of the orientation of the perturbation force vector corresponding to the following biomechanical effects: (i) an increase in step length without affecting step height (vector orientation =  $8^\circ$ ), (ii) a decrease in step length without affecting step height (vector orientation =  $180^\circ$ ), (iii) an increase in step height without affecting step length (vector orienta-

tion =  $35^\circ$ ), (iv) a decrease in step height without affecting step length (vector orientation =  $250^\circ$ ), (v) a maximal step-length deviation from baseline with a combined effect on step length and step height (vector orientation =  $140^\circ$ ), and (vi) a maximal step-height deviation from baseline with a combined effect on step length and step height (vector orientation =  $70^\circ$ ). We refer to these testing conditions as  $X$ ,  $X_{inv}$ ,  $Y$ ,  $Y_{inv}$ ,  $X_{max}$ , and  $Y_{max}$ , respectively. Figure 1 (C and D) shows a schematic representation of the perturbation force vectors corresponding to these testing conditions and their biomechanical effects.

### Motor adaptation experiments

Data were gathered over 240 gait cycles divided in three blocks of 80 gait cycles. During the first block, the robot was programmed to minimize the interaction forces between the subject and the robot (baseline phase). During the second block, the robot generated a perturbation force vector aimed to affect the trajectory of the right foot (perturbation phase). During the last block (aftereffect phase), the robot was programmed as during the baseline phase. This experimental protocol was repeated six times during two separate sessions to study subjects' motor adaptation in response to perturbation force vectors with the six abovementioned vector orientations.

These experiments were performed in a group of 15 study volunteers. Figures 2 to 4 show the step-length and step-height data collected during the motor adaptation experiments. To test whether

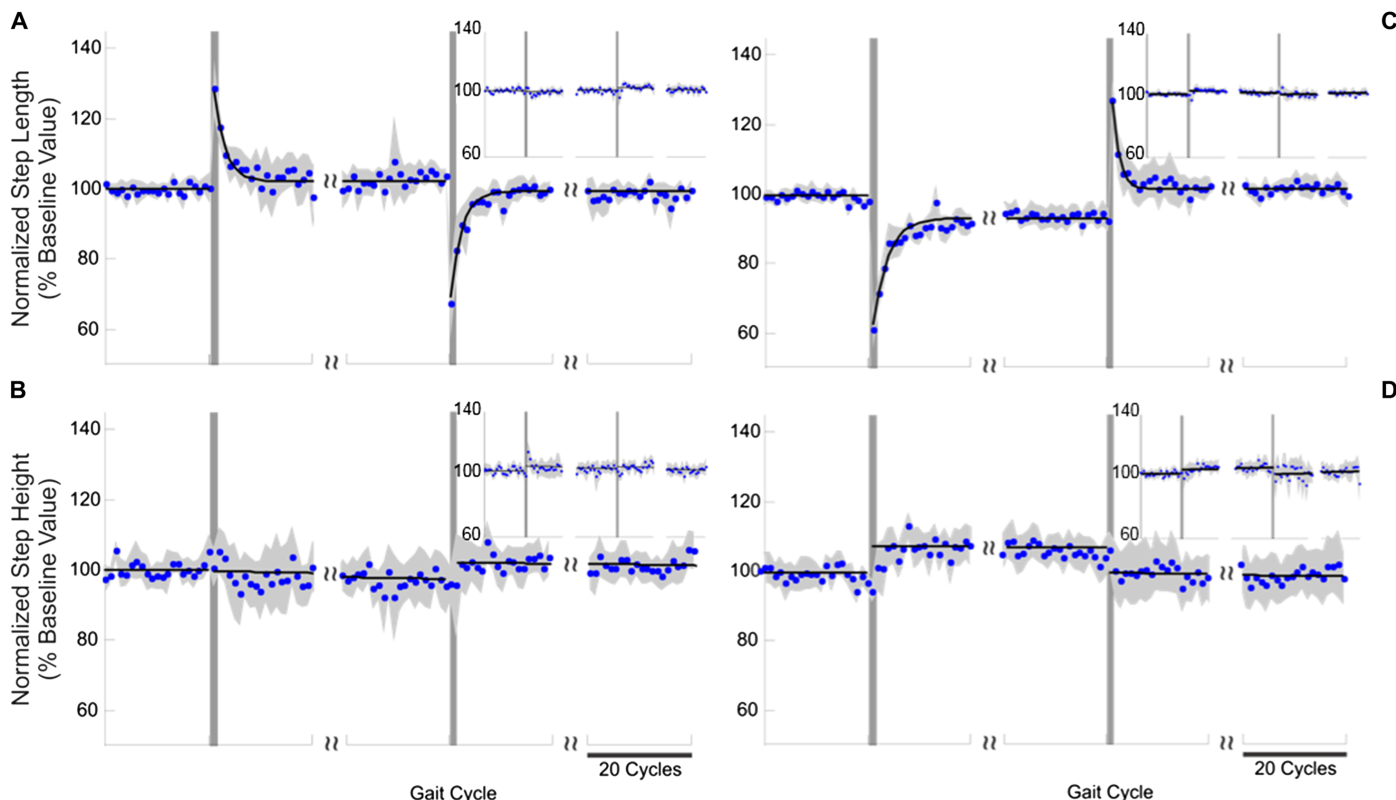


**Fig. 2. Results of the experiments in the  $X$  (A and B) and  $X_{inv}$  (C and D) testing conditions.** Step-length (A and C) and step-height (B and D) values observed during the experiments for the right lower limb (large plots) and the left lower limb (insets). The blue dots represent the average normalized step-length and step-height values (aggregate data across subjects), the gray shaded areas represent the SE, and the black solid line represents the line or exponential function best fitting the points for each phase of the experiment. The vertical lines represent the onset and end of the perturbation phase. The perturbation force vector generated by the robot during these experiments affected only the step length of the right lower limb. Motor adaptations are apparent for step length.

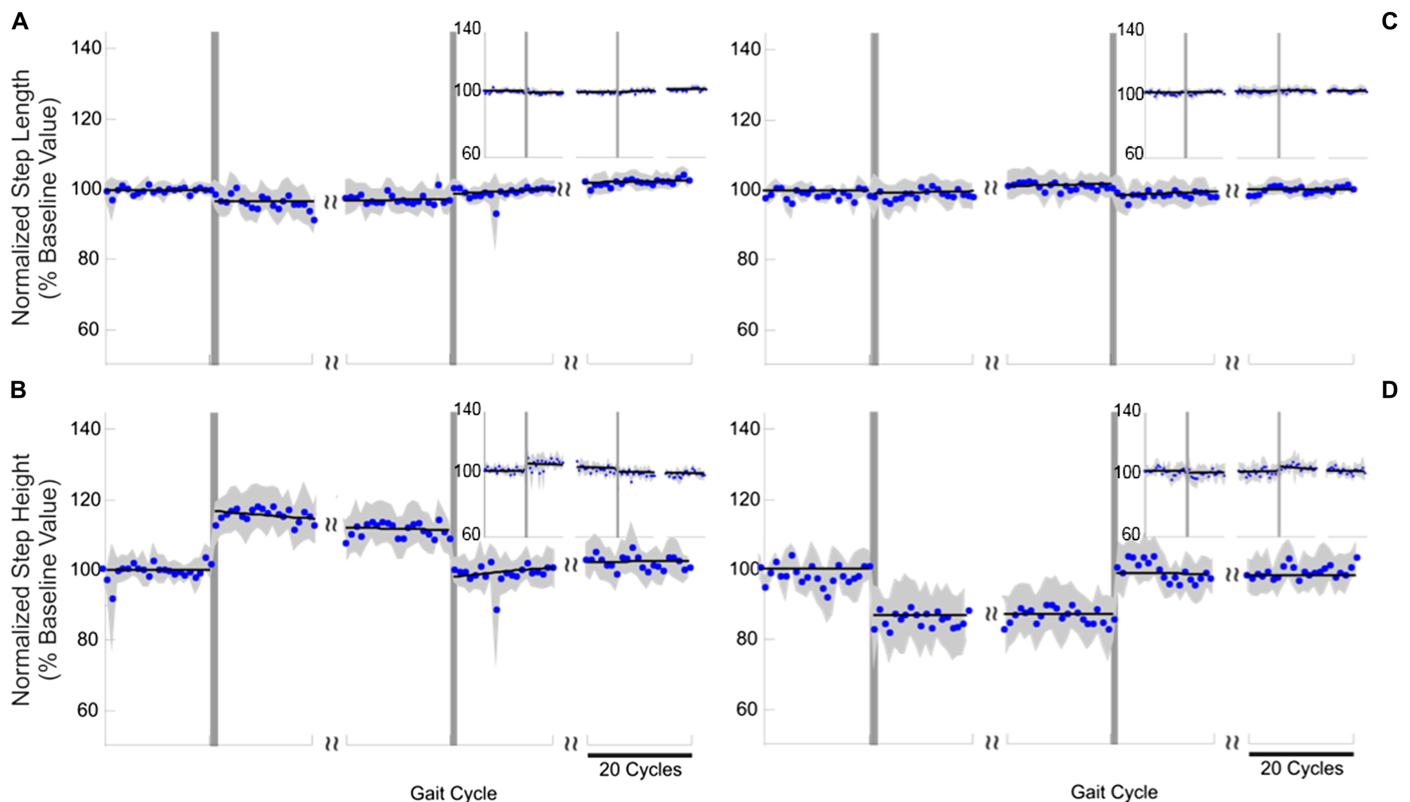


**Fig. 3. Results of the experiments in the  $Y$  (A and B) and  $Y_{inv}$  (C and D) testing conditions.** Step-length (A and C) and step-height (B and D) values observed during the experiments for the right lower limb (large plots) and the left lower limb (insets). The blue dots represent the average normalized step-length and step-height values (aggregate data across subjects), the gray shaded areas represent the SE, and the black solid line represents the line or exponential function best fitting the points for each phase of the experiment. The vertical lines represent the onset and end of the perturbation phase. The perturbation force vector generated by the robot during these experiments affected only the step height of the right lower limb. No motor adaptations are apparent in these plots.

step-length and step-height changes observed during the experiments were significant, we performed Friedman tests followed by post hoc analyses using the minimum significant difference test. The significance level  $\alpha$  was set to 0.05. Besides, an exponential function was used to fit the group data for each of the three phases of the experiments (baseline, perturbation, and aftereffect) in each testing condition and derive the time constants associated with behaviors observed for each of these phases. Details about the statistical analyses performed on the results of all testing conditions can be found in the Supplementary Materials.

#### **Adaptations to pure step-length perturbations**

We found that, when the robot produced a perturbation force vector that, by design, led to a significant increase or a decrease in step length without affecting step height (i.e.,  $X$  and  $X_{inv}$  conditions), subjects displayed systematic step-length motor adaptation that compensated for these perturbations. After the change in step length that occurred at the onset of the perturbation phase of the experiments, we observed a gradual but systematic return to the baseline step length (Fig. 2). Because the observed reductions in the kinematic effects of the perturbations could be caused by increased feedback corrections, limb stiffness, or predictive feed-forward motor adaptation, we examined the aftereffects that occurred when perturbations were withheld after training (i.e., the perturbation phase of the experiments). We found a remarkably close match between the aftereffect amplitude and the amount of perturbation compensation

observed during training. This observation indicates that the compensatory reduction of the displacement observed during the perturbation phase of the  $X$  and  $X_{inv}$  perturbation experiments is due to a predictive feed-forward motor adaptation. Exponential fitting of the results of these experiments provided estimates of the time constants associated with the time course of the motor behaviors that marked the perturbation and aftereffect phases of the experiments. We defined as steady state the step-length value reached at three times the value of the time constants for each of the abovementioned phases of the experiments. The results showed that about 10 gait cycles were needed to adapt to the perturbation force vector for both the  $X$  and  $X_{inv}$  perturbations. Aftereffects persisted for about seven gait cycles in both the  $X$  and  $X_{inv}$  perturbations.

#### **Adaptations to pure step-height perturbations**

In stark contrast to step-length perturbations, we found that subjects displayed little to no adaptive compensation when robot-generated perturbations led, by design, to an increase or a decrease in step height without affecting step length (i.e.,  $Y$  and  $Y_{inv}$  conditions). The results of these experiments are shown in Fig. 3. Step-height displacements observed during the first gait cycle after perturbation onset persisted for the duration of the perturbation phase of the experiments. Correspondingly, we found no aftereffects when the  $Y$  and  $Y_{inv}$  perturbations were withheld. These results indicate that there is little to no adaptation for perturbations that specifically increase or decrease step height. Comparison of the motor adaptation induced by pure step length

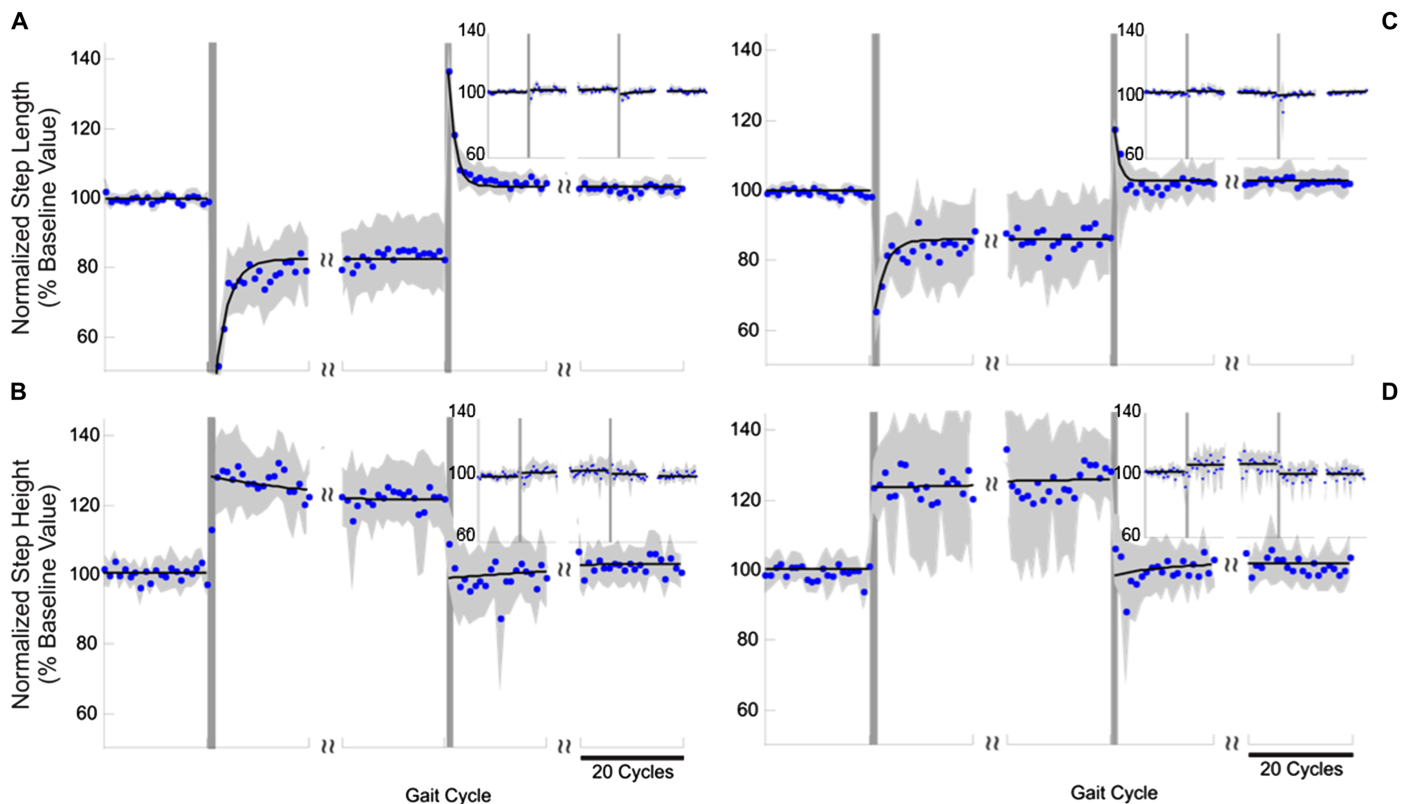


**Fig. 4. Results of the experiments in the  $X_{\max}$  (A and B) and  $Y_{\max}$  (C and D) testing conditions.** Step-length (A and C) and step-height (B and D) values observed during the experiments for the right lower limb (large plots) and the left lower limb (insets). The blue dots represent the average normalized step-length and step-height values (aggregate data across subjects), the gray shaded areas represent the SE, and the black solid line represents the line or exponential function best fitting the points for each phase of the experiment. The vertical lines represent the onset and end of the perturbation phase. The perturbation force vector generated by the robot during these experiments affected both the step length and the step height of the right lower limb. However, only motor adaptations to compensate for step-length changes are apparent in these plots.

( $X$  and  $X_{\text{inv}}$ ) versus pure step height ( $Y$  and  $Y_{\text{inv}}$ ) reveals that the human motor system adaptively compensates for external perturbations that affect step length but does not for perturbations that affect step height.

#### Adaptations to combined step-length and step-height perturbations

We investigated whether the contrast between no adaptation to step-height perturbations and strong adaptation to step-length perturbations would persist if these perturbations were simultaneously experienced. We thus applied gait perturbations that simultaneously affected step height and step length. We chose perturbation directions with maximal effect on step length and step height ( $X_{\max}$  and  $Y_{\max}$ ). Figure 4 shows the results of these experiments. During the perturbation phase in the  $X_{\max}$  condition, we observed a highly selective motor adaptation. At the end of the perturbation phase, we observed a significant adaptation in step length but little adaptation in step height. Besides, the step-length decrease observed during the first gait cycle of the perturbation phase was mirrored by a step-length increase during the first gait cycle of the aftereffect phase of the experiments, followed by a gradual, nearly complete return to baseline step length. In contrast, step height during the first gait cycle of the aftereffect phase showed no significant deviation from the baseline step-height value. The results of the experiments carried out in the  $Y_{\max}$  condition confirmed the observation from the experiments carried out in

the  $X_{\max}$  condition. Subjects showed motor adaptation to compensate for the effect of the perturbation on step length but not for the effect on step height. Study participants required about 15 gait cycles to adapt to the  $X_{\max}$  perturbation and about 23 gait cycles to adapt to the  $Y_{\max}$  perturbation. Aftereffects persisted for about nine gait cycles in the  $X_{\max}$  condition and for about 13 gait cycles in the  $Y_{\max}$  condition.

#### A selective process of generation of motor adaptation

Figure 5 summarizes the results for all testing conditions. The top panel shows the initial deviations (i.e., observed during the first gait cycle of the perturbation phase) in step length and step height caused by the mechanical perturbations. The middle panel shows the percentage of the initial deviations in step length and step height that study participants compensated for. The bottom panel shows the change in mechanical work observed in response to the perturbation force vector produced by the robot. The results are grouped by perturbations with effect only on step length (i.e., “step-length perturbations,”  $X$  and  $X_{\text{inv}}$ ), with effect only on step height (i.e., “step-height perturbations,”  $Y$  and  $Y_{\text{inv}}$ ), and with combined effects on step length and step height (i.e., “mixed perturbations,”  $X_{\max}$  and  $Y_{\max}$ ).

Table 1 shows the results of the statistical analyses (Wilcoxon’s signed-rank tests) that we performed to assess whether the magnitude of the adaptation was different from zero. Although significant step-length adaptations ( $P < 0.05$ ) were observed for all the testing

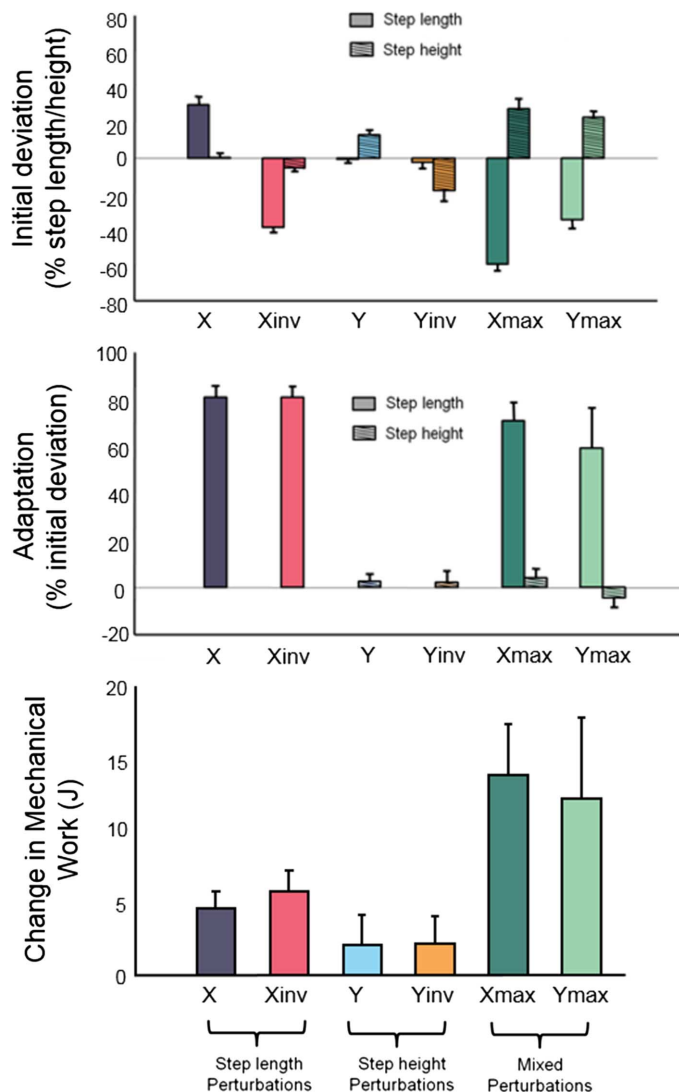


**Fig. 5. Summary of the results of the motor adaptation experiments. (Top)** Initial percentage deviation in step length and step height induced by each perturbation. **(Middle)** Magnitude of the observed motor adaptations. The data are shown as the percentage of the initial perturbation that subjects adapted to by the end of the perturbation phase of the experiment. **(Bottom)** Change in mechanical work between the last 10 steps of the baseline phase and the last 10 steps of the perturbation phase of the experiments. No motor adaptations in step height were ever observed. All the conditions that showed motor adaptations for step length were associated with a significant increase in work. Testing conditions during which motor adaptations were not observed showed no significant differences in net work between the baseline and the end of the perturbation phase.

conditions associated with a robot-induced change in step length (i.e.,  $X$ ,  $X_{inv}$ ,  $X_{max}$ , and  $Y_{max}$ ), no significant step-height adaptation was observed for the testing conditions associated with a robot-induced change in step height (i.e.,  $Y$ ,  $Y_{inv}$ ,  $X_{max}$ , and  $Y_{max}$ ). Table 1 also shows the results of Wilcoxon’s signed-rank tests that we performed to evaluate whether the work that study participants performed in response to the perturbation force vector produced by the robot was different from zero. Significant changes ( $P < 0.05$ ) were observed only for the perturbation conditions affecting step length. Subjects generated additional 5 to 15 J of work per gait cycle to counter the pertur-

**Table 1. Statistical analysis of the changes in step length and step height as well as the changes in net mechanical work observed during the perturbation phase of the experiments.  $**P < 0.01$ , Wilcoxon’s signed-rank test. n.a., not applicable.**

Testing condition	Adaptation		
	Step length	Step height	Mechanical work
$X$	<0.01**	n.a.	<0.01**
$X_{inv}$	<0.01**	n.a.	<0.01**
$Y$	n.a.	0.19	n.a.
$Y_{inv}$	n.a.	0.72	n.a.
$X_{max}$	<0.01**	0.12	<0.01**
$Y_{max}$	<0.01**	0.63	<0.01**

bations. Together, the results of these experiments demonstrate a notable selectivity whereby motor adaptation is observed for perturbations of step length but not step height, regardless of whether perturbations have an effect on step length and step height in isolation or in combination.

**DISCUSSION**

Our results revealed a selective process of generation of motor adaptation in response to robot-induced perturbations of human walking. Namely, motor adaptation was observed in response to changes in step length but not to changes in step height. What is the origin of this selective process? Previous studies have suggested three principles possibly underlying the generation of motor adaptation: (i) maintaining the baseline gait patterns, (ii) minimizing the metabolic cost of locomotion, and (iii) preserving locomotor stability.

**Preservation of locomotor stability**

Our results are at odds with the hypothesis that adaptation is driven solely by the aim of maintaining the baseline walking patterns because adaptations were not observed for perturbations in step height. The results are also at odds with the hypothesis that adaptation is driven solely by the objective of minimizing the metabolic cost of locomotion. The mechanical work generated by subjects in the  $X$ ,  $X_{inv}$ ,  $X_{max}$ , and  $Y_{max}$  conditions increased during the perturbation phase of the experiments as subjects countered the robot-induced perturbations. In contrast, the results are consistent with the hypothesis that motor adaptation aims to preserve locomotor stability. This explanation appears to account for the fact that subjects did not compensate for perturbations with effect on step height. Changes in step height of the magnitude tested in the study appear to be similar to those observed while negotiating an obstacle, a task that would not challenge the stability of human walking. Vice versa, step-length control is highly relevant to preserving locomotor stability. Stability boundaries during walking have been related to the position and velocity of the center of mass (CoM) relative to the base of support (BoS) (17). Several studies (18–22) have highlighted the importance of the placement of the foot on the ground at heel strike to maintain the projection of the CoM inside the BoS and thus preserve

Downloaded from https://www.science.org at The Hong Kong University of Science and Technology (Guangzhou) on May 27, 2026

locomotor stability (23). This concept has been applied to the control of bipedal robots (24–29). Furthermore, experiments in which healthy individuals were exposed to perturbations designed to challenge their balance during walking showed that subjects respond to perturbations by altering the trajectory of the CoM (30, 31) and/or the area of the BoS (32, 33). The former response is primarily achieved by modifying the position of the trunk, whereas the latter is mainly achieved by controlling the position of the foot on the ground at the time of heel strike. Furthermore, it has been shown that walking speed, cadence, and step length are jointly controlled to maximize locomotor stability (34). In our experiments, in which speed and cadence were controlled, motor adaptation restoring baseline step length would preserve the preferred relationships among walking speed, cadence, and step length.

### Locomotor stability over multiple steps

One could notice that study participants could not fall when strapped to the exoskeleton system used in our experiments. Also, the step-length changes caused by the robot in our experiments do not appear to be of a magnitude sufficient to cause an immediate loss of balance. Then, why would the CNS process the perturbations as challenging locomotor stability?

Previous studies with focus on the control of bipedal robots could provide the answer. Pratt and coauthors introduced the concept of  $N$ -step capture points and regions as a fundamental principle to enable long-term stability of bipedal robots and a stable  $N$ -step stopping strategy during robotic locomotion (26–28). In this framework, the stability of the bipedal robot is defined by the number of steps ( $N$ ) required to stop without falling.  $N$  strictly depends on foot placement for each step that the robot takes. By applying this conceptual framework to human walking, one would conclude that a mechanical perturbation that alters step length may affect the long-term (i.e., over multiple steps) stability of the subject even if the mechanical perturbation does not challenge the subject's immediate stability. Then, subjects would develop a motor plan to assure locomotor stability on the basis of the prediction of the effects of that perturbation over several gait cycles.

### Comparison with previous studies

At a first glance, our results appear to be in disagreement with previous studies by Emken and Reinkensmeyer (5) and van Asseldonk *et al.* (7), in which motor adaptation was observed in response to robot-induced changes in step height. However, in these studies, the authors used exoskeleton systems that differ in one fundamental aspect from the one that we used. While the robotic system that we used constrained the movement of the pelvis, the ones used in previous studies did not. We argue that, in the experiments performed by Emken and Reinkensmeyer (5) and van Asseldonk *et al.* (7), the mechanical perturbations generated by the robots caused movements of the pelvis and upper body, resulting in a significant acceleration of the CoM. We speculate that these mechanical perturbations were processed by the CNS as challenging the stability of locomotion, thus triggering the generation of motor adaptation. In this context, one would expect that perturbations causing a deviation from the baseline foot trajectory of large magnitude would produce a significant acceleration of the CoM and thus trigger a motor adaptation in response to the balance perturbation. In contrast, perturbations causing a deviation of small magnitude would not trigger a motor adaptation because they would not be processed as challenging locomotor

stability. These considerations are consistent with the results of the above-referenced studies. Conversely, the robotic system used in our experiments constrained the movement of the pelvis, hence preventing a significant acceleration of the CoM. Consequently, we did not observe any motor adaptation.

### Clinical implications

The experimental paradigm used in this study could result in the development of a method to assess the ability of patients undergoing rehabilitation to process and respond to perturbations generated by an exoskeleton system for robot-assisted treadmill-based gait rehabilitation. Such method would be of great interest in a clinical context if the ability of patients to process and respond to perturbations could be used to predict the responsiveness of each patient to robot-assisted gait training interventions. In addition, it would be of great interest to evaluate whether the paradigm proposed here could be used to assess the stability boundaries of individuals with motor impairments. If so, one could envision designing individualized gait training interventions driven by criteria such as the long-term stability of locomotion. Last, the results of this study suggest that motor adaptation can be leveraged only to change those aspects of patients' gait patterns that are processed by the CNS as challenging locomotor stability. We hypothesize that other feedback modalities would be necessary to induce changes in gait patterns along other dimensions.

## MATERIALS AND METHODS

### Study design

Two cohorts of subjects were recruited in the study. The first cohort of subjects was recruited to investigate the response to single-step perturbations. For this study, we recruited nine male and six female subjects, with an age of  $32.7 \pm 8.0$  years (mean  $\pm$  SD), weight of  $74 \pm 14$  kg, and height of  $174 \pm 11$  cm. The second cohort of subjects was recruited to investigate motor adaptation. For this study, we recruited 10 male and 5 female subjects, with an age of  $30.5 \pm 6.5$  years (mean  $\pm$  SD), weight of  $72 \pm 10$  kg, and height of  $174 \pm 9$  cm. Thirteen subjects participated in both sets of experiments.

The first set of experiments took place during a single session. Subjects underwent three trials. The first trial was performed to identify control settings that minimized the interaction forces between the subjects and the robotic legs using a method previously proposed by Vallery *et al.* (35). The second trial was performed to collect data that were later used to track the point of the gait cycle that subjects were at using an algorithm previously developed by Aoyagi *et al.* (36). During the third trial, we instructed subjects to walk for a period of time corresponding to the performance of 770 gait cycles. Subjects walked freely for the first 10 gait cycles. After that, we performed four blocks of 190 gait cycles each. During each block, we generated 19 single-step perturbations with 19 different orientation values of the perturbation force vector randomly selected among predefined values spanning the range from  $0^\circ$  to  $360^\circ$  by steps of  $20^\circ$ . Gait cycles randomly selected to produce a perturbation were marked by a minimum separation of five gait cycles and a maximum separation of eight gait cycles. For each orientation value of the perturbation force vector, we collected four data points, namely, one for each of the four blocks of 190 gait cycles. The four data points were averaged to generate a single data point per subject. The average and SE values estimated across subjects were used to derive the relationship between the orientation of the

perturbation force vector and the changes in step length and step height compared with baseline.

The motor adaptation experiments took place over two sessions. During each session, subjects underwent five trials. The first two trials were identical to the first two trials performed during the session devoted to the study of single-step perturbations. The following three trials were devoted to investigate motor adaptation. Subjects were instructed to walk for a period of time corresponding to the performance of 420 gait cycles for each trial. After the first 20 gait cycles, during which the robotic system was programmed to minimize the interaction forces between the subjects and the robot, we generated nine single-step perturbations over randomly selected gait cycles out of 160 gait cycles. Gait cycles during which a mechanical perturbation was applied were separated by a minimum of eight gait cycles. The remaining 240 gait cycles of each trial were divided into three blocks of 80 gait cycles. Each of these three blocks consisted of the baseline, perturbation, and aftereffect phases of the motor adaptation experiments described above. All perturbations within a trial were marked by the same orientation of the perturbation force vector.

### Data analysis

Step length was defined as the maximum value of the foot position in the anteroposterior direction in a coordinate system positioned at the center of rotation of the robotic joint connecting the pelvis and thigh components of the exoskeleton system. Step height was defined as the distance between the foot and the belt of the treadmill during the midswing phase of the gait cycle. This definition of step height allowed us to measure it where the effect of the perturbation led to a maximum deviation from the baseline value.

Step-length and step-height data collected during the single-step perturbations were analyzed to determine the relationship between the orientation of the perturbation force vector and the magnitude of the changes in step length and step height observed in response to the perturbations. The experimental data points were interpolated using cubic splines to determine the orientation values of the perturbation force vector corresponding to the six conditions described in Results. These orientation values were used in the motor adaptation experiments.

Step-length and step-height values were estimated for different phases of the motor adaptation experiments. Specifically, we estimated the following step-length and step-height values: (i) average during the baseline phase, (ii) value for the first gait cycle of the perturbation phase, (iii) value for the last gait cycle of the perturbation phase, (iv) value for the first gait cycle of the aftereffect phase, and (v) value for the last gait cycle of the aftereffect phase. Statistical comparisons among the above-listed step-length and step-height values were performed using Friedman tests followed by post hoc analyses using the minimum significant difference test (see the Supplementary Materials). Besides, we estimated the magnitude of the adaptation as the percentage of the initial deviation that was compensated for at the end of the perturbation phase. This analysis was performed for step length and step height when statistically significant differences were observed between the value observed at baseline and the value observed for the first step of the perturbation phase of the experiments. Wilcoxon's signed-rank tests were performed to assess whether the magnitude of the adaptation was different from zero. Mechanical work was estimated from the angular displacements and the interaction torques recorded by the exoskel-

eton at the hip and the knee (see the Supplementary Materials for details). Wilcoxon's signed-rank tests were performed to estimate differences in mechanical work between the baseline phase and the last 10 steps of the perturbation phase for conditions showing motor adaptation. The significance level  $\alpha$  was set to 0.05 for all the tests described above.

### SUPPLEMENTARY MATERIALS

robotics.sciencemag.org/cgi/content/full/2/6/eaam7749/DC1

Text

Fig. S1. Schematic representation of the motor adaptation experiments.

Fig. S2. Comparison of the robot joint angles during the baseline phase of the experiments and normative joint angle data collected during overground walking.

Fig. S3. Comparison of joint interaction torque and power values during the baseline phase of the experiments and normative data collected during overground walking.

Fig. S4. Diagram of the controller of the exoskeleton.

Fig. S5. Effect of the metronome on the variability in the ankle velocity.

Fig. S6. Kinematics and kinetics of motion for the right lower limb during all testing conditions.

Fig. S7. Kinematics and kinetics of motion for the left lower limb during all testing conditions.

Fig. S8. Aggregate results for changes in step length and step height for the  $X$  testing condition.

Fig. S9. Aggregate results for changes in step length and step height for the  $X_{inv}$  testing condition.

Fig. S10. Aggregate results for changes in step length and step height for the  $Y$  testing condition.

Fig. S11. Aggregate results for changes in step length and step height for the  $Y_{inv}$  testing condition.

Fig. S12. Aggregate results for changes in step length and step height for the  $X_{max}$  testing condition.

Fig. S13. Aggregate results for changes in step length and step height for the  $Y_{max}$  testing condition.

Table S1. Statistical analysis to test for step-length and step-height differences observed during the motor adaptation experiments for all testing conditions.

Table S2. Time constants of adaptation calculated from the aggregate data (mean  $\pm$  SE).

Table S3. Comparisons of the values of the time constants derived from individual data associated with motor adaptation for the  $X$ ,  $X_{inv}$ ,  $X_{max}$  and  $Y_{max}$  testing conditions.

Table S4. Analysis of the symmetry indices for step length, step height, and the net mechanical work generated by subjects during the baseline and perturbation phases of the motor adaptation experiments.

References (37–39)

### REFERENCES AND NOTES

1. R. Shadmehr, F. A. Mussa-Ivaldi, Adaptive representation of dynamics during learning of a motor task. *J. Neurosci.* **14**, 3208–3224 (1994).
2. D. M. Wolpert, R. C. Miall, Forward models for physiological motor control. *Neural Netw.* **9**, 1265–1279 (1996).
3. M. Kawato, Internal models for motor control and trajectory planning. *Curr. Opin. Neurobiol.* **9**, 718–727 (1999).
4. K. A. Thoroughman, R. Shadmehr, Learning of action through adaptive combination of motor primitives. *Nature* **407**, 742–747 (2000).
5. J. L. Emken, D. J. Reinkensmeyer, Robot-enhanced motor learning: Accelerating internal model formation during locomotion by transient dynamic amplification. *IEEE Trans. Neural Syst. Rehabil. Eng.* **13**, 33–39 (2005).
6. J. L. Emken, R. Benitez, A. Sideris, J. E. Bobrow, D. J. Reinkensmeyer, Motor adaptation as a greedy optimization of error and effort. *J. Neurophysiol.* **97**, 3997–4006 (2007).
7. E. H. F. van Asseldonk, B. Koopman, H. van der Kooij, Locomotor adaptation and retention to gradual and sudden dynamic perturbations, 2011 IEEE International Conference on Rehabilitation Robotics, Zurich, Switzerland, 29 June to 1 July 2011 (IEEE, 2011).
8. I. Cajigas, M. T. Goldsmith, A. Duschau-Wicke, R. Riener, M. A. Smith, E. N. Brown, P. Bonato, Assessment of lower extremity motor adaptation via an extension of the force field adaptation paradigm. *Conf. Proc. IEEE Eng. Med. Biol. Soc.* **2010**, 4522–4525 (2010).
9. T. Lam, M. Anderschitz, V. Dietz, Contribution of feedback and feedforward strategies to locomotor adaptations. *J. Neurophysiol.* **95**, 766–773 (2006).
10. J. C. Selinger, S. M. O'Connor, J. D. Wong, J. M. Donelan, Humans can continuously optimize energetic cost during walking. *Curr. Biol.* **25**, 2452–2456 (2015).
11. T. Prokop, W. Berger, W. Zijlstra, V. Dietz, Adaptational and learning processes during human split-belt locomotion: Interaction between central mechanisms and afferent input. *Exp. Brain Res.* **106**, 449–456 (1995).

12. D. S. Reisman, H. J. Block, A. J. Bastian, Interlimb coordination during locomotion: What can be adapted and stored? *J. Neurophysiol.* **94**, 2403–2415 (2005).
13. J. T. Choi, A. J. Bastian, Adaptation reveals independent control networks for human walking. *Nat. Neurosci.* **10**, 1055–1062 (2007).
14. D. N. Savin, S.-C. Tseng, S. M. Morton, Bilateral adaptation during locomotion following a unilaterally applied resistance to swing in nondisabled adults. *J. Neurophysiol.* **104**, 3600–3611 (2010).
15. J. M. Finley, A. J. Bastian, J. S. Gottschall, Learning to be economical: The energy cost of walking tracks motor adaptation. *J. Physiol.* **591**, 1081–1095 (2013).
16. A. J. Bastian, Understanding sensorimotor adaptation and learning for rehabilitation. *Curr. Opin. Neurol.* **21**, 628–633 (2008).
17. Y.-C. Pai, J. Patton, Center of mass velocity-position predictions for balance control. *J. Biomech.* **30**, 347–354 (1997).
18. A. L. Hof, The ‘extrapolated center of mass’ concept suggests a simple control of balance in walking. *Hum. Mov. Sci.* **27**, 112–125 (2008).
19. A. E. Patla, Strategies for dynamic stability during adaptive human locomotion. *IEEE Eng. Med. Biol. Mag.* **22**, 48–52 (2003).
20. D. A. Winter, Human balance and posture control during standing and walking. *Gait Posture* **3**, 193–214 (1995).
21. D. A. Winter, Sagittal plane balance and posture in human walking. *IEEE Eng. Med. Biol. Mag.* **6**, 8–11 (1987).
22. J. Perry, J. Burnfield, *Gait Analysis: Normal and Pathological Function* (Slack Incorporated, 2010).
23. A. L. Hof, M. G. J. Gazendam, W. E. Sinke, The condition for dynamic stability. *J. Biomech.* **38**, 1–8 (2005).
24. H. Geyer, H. Herr, A muscle-reflex model that encodes principles of legged mechanics produces human walking dynamics and muscle activities. *IEEE Trans. Neural Syst. Rehabil. Eng.* **18**, 263–273 (2010).
25. S. Kajita, F. Kanehiro, K. Kaneko, K. Yokoi, H. Hirukawa, The 3D linear inverted pendulum mode: A simple modeling for a biped walking pattern generation. *Proceedings of the IEEE/RSJ International Conference on Intelligent Robots and Systems*, Maui, HI, 29 October to 3 November 2001 (IEEE, 2001).
26. T. Koolen, T. de Boer, J. Rebula, A. Goswami, J. Pratt, Capturability-based analysis and control of legged locomotion, Part 1: Theory and application to three simple gait models. *Int. J. Robot Res.* **31**, 1094–1113 (2012).
27. J. Pratt, T. Koolen, T. De Boer, J. Rebula, S. Cotton, J. Carff, M. Johnson, P. Neuhaus, Capturability-based analysis and control of legged locomotion, Part 2: Application to M2V2, a lower-body humanoid. *Int. J. Robot Res.* **31**, 1117–1133 (2012).
28. J. E. Pratt, R. Tedrake, Velocity-based stability margins for fast bipedal walking, in *Fast Motions in Biomechanics and Robotics* (Springer, 2006), vol. 340, pp. 299–324.
29. M. A. Townsend, Biped gait stabilization via foot placement. *J. Biomech.* **18**, 21–38 (1985).
30. R. F. Reynolds, A. M. Bronstein, The broken escalator phenomenon. Aftereffect of walking onto a moving platform. *Exp. Brain Res.* **151**, 301–308 (2003).
31. J.-Y. You, Y.-L. Chou, C.-J. Lin, F.-C. Su, Effect of slip on movement of body center of mass relative to base of support. *Clin. Biomech.* **16**, 167–173 (2001).
32. R. Cham, M. S. Redfern, Lower extremity corrective reactions to slip events. *J. Biomech.* **34**, 1439–1445 (2001).
33. R. Cham, M. S. Redfern, Changes in gait when anticipating slippery floors. *Gait Posture* **15**, 159–171 (2002).
34. M. D. Latt, H. B. Menz, V. S. Fung, S. R. Lord, Walking speed, cadence and step length are selected to optimize the stability of head and pelvis accelerations. *Exp. Brain Res.* **184**, 201–209 (2008).
35. H. Vallery, A. Duschau-Wicke, R. Riener, Generalized elasticities improve patient-cooperative control of rehabilitation robots, 2009 *IEEE International Conference on Rehabilitation Robotics*, Kyoto, Japan, 23 to 26 June 2009 (IEEE, 2009).
36. D. Aoyagi, W. E. Ichinose, S. J. Harkema, D. J. Reinkensmeyer, J. E. Bobrow, A robot and control algorithm that can synchronously assist in naturalistic motion during body-weight-supported gait training following neurologic injury. *IEEE Trans. Neural Syst. Rehabil. Eng.* **15**, 387–400 (2007).
37. R. Riener, L. Lünenburger, I. C. Maier, G. Colombo, V. Dietz, Locomotor training in subjects with sensori-motor deficits: An overview of the robotic gait orthosis lokomat. *J. Healthc. Eng.* **1**, 197–216 (2010).
38. A. Duschau-Wicke, J. von Zitzewitz, A. Caprez, L. Lunenburger, R. Riener, Path control: A method for patient-cooperative robot-aided gait rehabilitation. *IEEE Trans. Neural Syst. Rehabil. Eng.* **18**, 38–48 (2010).
39. R. A. Scheidt, M. A. Conditt, E. L. Secco, F. A. Mussa-Ivaldi, Interaction of visual and proprioceptive feedback during adaptation of human reaching movements. *J. Neurophysiol.* **93**, 3200–3213 (2005).

**Acknowledgments:** We would like to thank A. Duschau-Wicke, R. Riener, H. Vallery, and the R&D team at Hocoma AG for providing access to software algorithms utilized to control the robotic system used in the study. **Funding:** This project was partially supported by the Wyss Institute for Biologically Inspired Engineering at Harvard University. I.C. was partially supported by the National Institute of Neurological Disorders and Stroke (award no. 1F31NS058275-01A2). A.K. was partially supported by the Swiss National Science Foundation (award no. PBEZ3\_137336). **Author contributions:** I.C., A.K., and G.S. contributed to the study design, performance of the experiments, analysis of the results, and writing of the manuscript. M.S. and P.B. contributed to the study design, analysis of the results, and writing of the manuscript. **Competing interests:** The authors declare that they have no competing financial interests. **Data and materials availability:** Please contact P.B. to obtain a copy of the data collected during the study.

Submitted 15 January 2017  
 Accepted 28 April 2017  
 Published 24 May 2017  
 10.1126/scirobotics.aam7749

**Citation:** I. Cajigas, A. Koenig, G. Severini, M. Smith, P. Bonato, Robot-induced perturbations of human walking reveal a selective generation of motor adaptation. *Sci. Robot.* **2**, eaam7749 (2017).

## Robot-induced perturbations of human walking reveal a selective generation of motor adaptation

Iahn Cajigas, Alexander Koenig, Giacomo Severini, Maurice Smith, and Paolo Bonato

*Sci. Robot.* **2** (6), eaam7749. DOI: 10.1126/scirobotics.aam7749

### View the article online

<https://www.science.org/doi/10.1126/scirobotics.aam7749>

### Permissions

<https://www.science.org/help/reprints-and-permissions>

Use of this article is subject to the [Terms of service](#)

---

*Science Robotics* (ISSN 2470-9476) is published by the American Association for the Advancement of Science, 1200 New York Avenue NW, Washington, DC 20005. The title *Science Robotics* is a registered trademark of AAAS.

Copyright © 2017, American Association for the Advancement of Science